PHOTOSYNTHETICA
International Journal for Photosynthesis Research

DOI 10.32615/ps.2024.038 PHOTOSYNTHETICA 62 (4): 381-392, 2024

Chloroplast antioxidant reactions associated with zinc-alleviating effects on iron toxicity in wheat seedlings

Y.L. XU†, J.Y. GUO†, Z. ZHANG, R.R. MA, H. MA, Y. ZHANG, and Y.L. YANG+

College of Life Science, Northwest Normal University, 730070 Lanzhou, China

Abstract

This study aimed to explore the mechanism by which Zn retards Fe toxicity by analyzing the morphological, photosynthetic, and chloroplast physiological parameters of wheat seedlings treated with either single or combined Zn and Fe. Different behavior of the seedlings was observed under untreated and treated conditions. The most discriminating quantitative traits were associated with leaf area, biomass dry mass and fresh mass, net photosynthetic rate, intercellular CO_2 concentration, stomatal conductance, transpiration rate of seedlings, Hill reaction, Mg^{2+}-ATPase and Ca^{2+}-ATPase activities, malondialdehyde and $O_2^{\bullet-}$ contents, and glutathione reductase, ascorbate peroxidase, peroxidase, and superoxide dismutase activities and their gene expression in the seedling chloroplast. The obtained findings suggest the important function of an appropriate Zn concentration in preventing Fe toxicity. Therefore, a thorough evaluation of the effects of Zn on Fe-stressed plant growth is beneficial for sustainable agriculture.

Keywords: antioxidant reaction; chloroplast; Fe stress; wheat; Zn treatment.

Introduction

With the rapid advancement of industrialization and urbanization and inadequate agricultural practices, soil contamination by heavy metals has escalated significantly. This predicament is particularly pronounced in agricultural soil, leading to dire consequences for crop health. The 2014 National Soil Pollution Survey Bulletin reveals an alarming heavy metal Zn occurrence rate of 0.9% in China. In Madagascar, the whole east coast has a high fraction of 'Fe-rich soils', and the total estimated area with 'Fe-rich soils' in Africa is 427 Mha (van Oort 2018). Despite being essential trace elements, excessive Zn or Fe contents in plants result in the emergence of necrotic spots and leaf chlorosis. Eventually, these conditions can impede plant growth and in severe cases, culminate in plant fatality (Krohling *et al*. 2016, Du *et al*. 2019, Gindri *et al*. 2020, Tisarum *et al*. 2023).

Chloroplasts serve as organelles crucial for photosynthesis, facilitating carbohydrate synthesis. Zn functions as a cofactor for certain enzymes engaged in chlorophyll (Chl) synthesis and the regulated assimilation of carbon dioxide (CO_2) in higher plants (Marschner 2012). Fe plays a pivotal role in sustaining chloroplast ultrastructure, function, and the metabolism of photosynthetic pigments (Briat *et al*. 2015, Mira *et al*. 2021,

Highlights

- Antioxidant responses in wheat chloroplasts were related to Fe toxicity
- Zn application relieved Fe toxicity through increasing chloroplast ATPase activity
- Antioxidant enzyme activity was regulated by ROS generation in wheat chloroplast

Received 29 February 2024
Accepted 4 November 2024
Published online 5 December 2024

+Corresponding author
phone: +86-13893632661
e-mail: xbsfxbsdyang@163.com

Abbreviations: APX – ascorbate peroxidase; Chl – chlorophyll; C_i – intercellular CO_2 concentration; DM – dry mass; DTT – dithiothreitol; E – transpiration rate; EDTA-Na_2 – ethylenediaminetetraacetic acid disodium salt; FM – fresh mass; GR – glutathione reductase; g_s – stomatal conductance; MDA – malondialdehyde; NBT – nitroblue tetrazolium; PBS – phosphate saline buffer; P_N – net photosynthetic rate; POD – peroxidase; ROS – reactive oxygen species; SOD – superoxide dismutase; TBA – thiobarbituric acid; TCA – trichloroacetic acid.

Acknowledgements: This work was financially supported by the National Natural Science Foundation of China (No.32160749).

†These authors contributed equally to this work.

Conflict of interest: The authors declare that they have no conflict of interest.

Müller 2023). Zn accumulates predominantly within chloroplasts and plant cell vacuoles, and leaf cell Fe is localized in chloroplasts (Chatterjee *et al*. 1996, Kroh and Pilon 2020). However, excessive exposure to Zn or Fe stress diminishes the photosynthetic rate and stomatal conductance, concurrent with reduced photosynthetic pigment concentrations within plants (Delias *et al*. 2022, Li *et al*. 2022). When plants confront heavy metal stressors, an intrinsic response is an overabundance of ROS accumulation, resulting in oxidative damage. ROS production primarily transpires within chloroplasts (Li and Kim 2022). Under unfavorable environmental conditions, an overproduction of ROS within chloroplasts can exacerbate damage by fostering the oxidation of target proteins and the peroxidation of membrane lipids (Li and Kim 2022). The enzymatic antioxidant system within chloroplasts comprises peroxidase (POD), glutathione reductase (GR), ascorbate peroxidase (APX), and superoxide dismutase (SOD) to counteract excessive ROS build-up, orchestrating ROS metabolism equilibrium. Exposure to heavy metal chromium stress significantly enhances APX, GR, and SOD activities within maize seedling chloroplasts (Dai and Shan 2019). This enhancement effectively mitigates the overproduction of ROS within chloroplasts, thereby preventing lipid peroxidation and pigment photooxidation. Consequently, this mechanism alleviates the impediments to CO_2 fixation within wheat by averting inhibition (Ding *et al*. 2017).

Although plant growth and physiological responses to heavy metal stress have garnered considerable attention, there is a noticeable dearth of studies examining the impact of Zn-induced effects or Fe toxicity on the physiological properties of chloroplasts. Recently, there has been an emerging recognition of Zn's ability to relieve heavy metal toxicity including Cd. Notably, applying Zn through leaf spraying has proven effective in reducing the Cd content in wheat grown on Cd-contaminated soils. This treatment also amplifies the enzymatic antioxidant defense system, leading to favorable wheat growth even under Cd stress conditions (Wu *et al*. 2019). Additionally, Zn supplementation has been found to counteract Cd toxicity by regulating ROS equilibrium in rice plants (Adil *et al*. 2020). Furthermore, Zn's presence enhances the resistance of *Cosmos bipinnatus* to Cd stress by stimulating antioxidative enzyme activities (Du *et al*. 2020). Our prior investigation demonstrated a substantial increase in hydrogen peroxide (H_2O_2) and malondialdehyde (MDA) contents in wheat roots with rising exogenous Fe concentrations (100, 300, and 500 μM). This increase coincided with a noteworthy reduction in Chl content in leaves, significantly impeding the growth and development of wheat seedlings (Li *et al*. 2012). Furthermore, we observed that a low Zn concentration could significantly ameliorate Fe toxicity by modulating the antioxidant response within wheat roots (Ma *et al*. 2017). Although the Zn-alleviating effect on plant heavy metal toxicity has received much attention from researchers, an in-depth exploration of its mechanism is lacking. In particular, the relationship between chloroplast's physiological characteristics and Zn's retarding effects on heavy metal toxicity in plants has remained unclear. Consequently, the present experiment involved treating *Triticum aestivum* L. cultivar Xihan3 seedlings with Zn, Fe, or a combination of both. Our goal was to determine the physiological response of chloroplasts and elucidate the regulatory mechanisms underlying Zn's capacity to alleviate Fe toxicity. This study offers insights into the biological assessment of heavy metal pollution and the foundation for future scientific evaluations.

Materials and methods

Cultivation and treatment of wheat seedlings: Wheat Xihan3 seeds bred by Gansu Agricultural University were sterilized by soaking in NaClO (1%, v/v) for 15 min, rinsed, and soaked overnight to fully absorb water, and germinated in darkness at 25°C for 24 h. Fully germinated seeds were selected and cultured in an incubator at 25°C and 300 μmol(photon) m^{-2} s^{-1} light/dark (12/12 h). Seedlings in the control group were grown in small plastic beakers containing 1/4 Hoagland nutrient solution. The treatment groups were established with 50 μM $ZnCl_2$, 250 μM $ZnCl_2$, 300 μM $FeCl_3$, 500 μM $FeCl_3$, 300 μM $FeCl_3$ + 50 μM $ZnCl_2$, 300 μM $FeCl_3$ + 250 μM $ZnCl_2$, and $ZnCl_2$ and/or $FeCl_3$ dissolved in 1/4 Hoagland nutrient solution. The culture solution was renewed every 48 h, and six-day-old seedlings were collected to detect the relevant indexes. To detect leaf area, 15 seedlings growing for 6 d were randomly selected from each beaker and washed with deionized water. Subsequently, the length and width of the long leaves were determined. Wheat leaf area = 0.78 × leaf length × leaf width. Additionally, the biomass of 20 seedlings with relatively uniform growth from each beaker was determined. These seedlings were washed with distilled water, and their stems and roots were used separately to determine fresh mass (FM). The stems and roots were dried at 80°C until their mass remained the same, and the dry mass (DM) was recorded.

Photosynthetic gas-exchange parameters: The midsection of the longleaf was placed in a gas-exchange cuvette (2 cm × 3 cm). Net photosynthetic rate (P_N), transpiration rate (E), stomatal conductance (g_s), and intercellular CO_2 concentration (C_i) were recorded by *Li-6400* portable device (*LiCor*, Lincoln, NE, USA) when the values were stable. The following parameters were set: light intensity of 800 μmol(photon) m^{-2} s^{-1}, gas flow rate of 300 μmol s^{-1}, and CO_2 concentration of 400 μmol mol^{-1}. Moreover, 15 leaves from each group were used to analyze these photosynthetic parameters.

Superoxide radical ($O_2^{\bullet-}$) **staining of wheat leaves**: We used the method of Kaur *et al*. (2016) for $O_2^{\bullet-}$ staining of wheat leaves. Leaf tips (3 cm) were cut from wheat leaves with similar shape, size, and morphology, and stained with 0.2 mmol L^{-1} nitroblue tetrazolium (NBT) solution dissolved in 50 mmol L^{-1} phosphate saline buffer (PBS) for 48 h away from light. Then, the leaf surface was rinsed with ddH_2O. The stained leaves were immersed in 95% ethanol and boiled for 1 h (100°C) until the green

background of the leaf was removed. The stained leaf was preserved in 50% glycerol or observed with a *Leica DFC 7000 T* microscope (Germany) and photographed.

Isolation and preparation of chloroplasts: The chloroplast isolation method was based on the slightly modified procedure outlined by Romanowska *et al*. (2006). Fresh leaves of 60 g were placed in 300 mL of chloroplast extract buffer consisting of 50 mM Hepes-KOH (pH 8.0), 330 μM sorbitol, 2.0 mM ethylenediaminetetraacetic acid disodium salt (EDTA-Na_2), 0.1% bovine serum albumin, 2 mM ascorbic acid, and 2 mM $MgCl_2$. Subsequently, leaves were homogenized for 15 s, with three repeated cycles, and filtered through six layers of gauze. Centrifugation was conducted at 700 × *g* for 5 min and 3,000 × *g* for 10 min, and the resultant precipitate was resuspended with a small quantity of chloroplast extraction buffer. Layers of 60, 45, and 30% sucrose were used to create a sucrose density gradient. About 2 mL of the chloroplast suspension was carefully placed onto this gradient. Following ultrafast centrifugation at 30,000 × *g* for 2 h, the green bands present at the interface of the 60 and 45% sucrose gradients were recovered. These bands were then resuspended in a volume of chloroplast extract buffer five times their volume. Further centrifugation for 10 min was performed at 3,000 × *g*, and the residual chloroplast suspension was carefully collected.

Chlorophyll content: The chloroplast suspension (0.1 mL) was mixed with 4.9 mL acetone (80%), and this mixture was shaken and centrifuged for 2 min (1,000 × *g*). The absorbance of the supernatant at 652 nm was recorded by ultraviolet visible spectrophotometry (*UV-2700*, *Shimadzu Instrument Co.*, *Ltd.*, China) and the Chl content was calculated referring to the description of Zhang *et al.* (2009).

Chloroplast Hill reaction activity: An appropriate volume of chloroplast extract (containing 20–40 μg of Chl) was introduced into 1 mL of the Hill reaction solution, comprising 50 mM Tris-HCl buffer (pH 7.6), 2 mM $K_3[Fe(CN)_6]$, and 5 mM $MgCl_2$. Following 1 min of light irradiation, the reaction was promptly terminated using 0.2 mL of trichloroacetic acid (TCA, 20%). The resulting supernatant (0.3 mL), obtained by centrifugation at 1,000 × *g* for 2 min, was added to 1.4 mL of water. Subsequently, 2 mL of a solution containing 0.2 mM sodium citrate, 100 μL of 10 mM $FeCl_3$, and 200 μL of 50 mM 1,10-phenanthroline hydrochloride were added. After thorough agitation and 10 min of incubation away from light, the absorbance at 520 nm was measured by ultraviolet visible spectrophotometry (*UV-2700*, *Shimadzu Instrument Co.*, *Ltd.*, China). A blank control without potassium ferrocyanide was used for reference. The Hill reaction activity, represented in terms of μmol $K_3[Fe(CN)_6]$ mg^{-1}(Chl) h^{-1}, was deduced using the standard curve established with potassium ferrocyanide.

Chloroplast Mg^{2+}-ATPase and Ca^{2+}-ATPase activities: The reaction system designed for determining chloroplast Mg^{2+}-ATPase (EC 3.6.1.3) activity comprised 100 μL of chloroplast suspension, 800 μL of 50 mM Tris-HCl (pH 8.0), 100 μM sodium chloride (NaCl), 10 mM $MgCl_2$ and 10 mM dithiothreitol (DTT). After 5 min of illumination, 100 μL of 100 μM adenosine triphosphate (ATP) was introduced, followed by incubation at 37°C incubation for 10 min. The detection method for chloroplast Ca^{2+}-ATPase (EC 3.6.3.8) activity consisted of 20 mM ATP, 50 mM Tris-HCl buffer (pH 8.0), and 5 mM DTT. A mixture comprising 800 μL of detection buffer and 100 μL of chloroplast suspension was heated for 4 min (64°C), after which this system was kept at room temperature. Subsequently, 10 mM ATP (100 μL) was added, and incubation (37°C) was maintained for 10 min. Following the incubation for the Mg^{2+}-ATPase and Ca^{2+}-ATPase activity detection systems, 200 μL of 20% TCA solution was introduced to terminate the reaction. After shaking and subsequent centrifugation (4,000 × *g*), 500 μL of the resulting supernatant was mixed with 2 mL of a ferrous sulfate ammonium molybdate reagent and 2.5 mL of distilled water. After 30 min of incubation, the absorbance at 660 nm was recorded by ultraviolet visible spectrophotometry (*UV-2700*, *Shimadzu Instrument Co.*, *Ltd.*, China). The phosphorus standard curve was employed to determine ATPase activity expressed as μmol(Pi) mg^{-1}(Chl) h^{-1} (Wang *et al*. 2010).

Chloroplast H_2O_2 content and $O_2^{\bullet-}$ production rate: Chloroplast H_2O_2 contents were assessed following the procedure described by Omoto *et al*. (2013) with some modifications. A chloroplast suspension (1 mL) containing an equivalent amount of Chl was mixed with 100 μL of concentrated HCl containing 20% titanium tetrachloride and 200 μL of concentrated ammonia. The mixture was centrifuged (1,000 × *g*) for 10 min, and acetone solution was employed to rinse the pigment adhering to the precipitate. It was then dissolved in 3 mL of 1 mM sulfuric acid. The H_2O_2 content was calculated and expressed as μmol mg^{-1}(Chl) based on the absorbance at 410 nm.

Chloroplast $O_2^{\bullet-}$ contents were evaluated following the method reported by Sharma *et al*. (2022) with slight modification. A chloroplast suspension with an equivalent Chl quantity (30 μg of Chl) was combined with 65 mM PBS buffer (pH 7.8, 675 μL) and hydroxylamine hydrochloride solution (10 mM, 100 μL). After 20 min of incubation (25°C), 375 μL of p-aminobenzene sulfonamide (17 mM) and 375 μL of α-naphthalamine (7 mM) were added. The mixed solution was maintained at 25°C for another 20 min. Finally, an equal volume of pure diethyl ether was added, and the rate of $O_2^{\bullet-}$ production, represented as μmol mg^{-1}(Chl) min^{-1}, was determined based on the absorbance at 530 mM using the sodium nitrite standard curve.

MDA content: MDA contents in wheat leaves and chloroplast were determined based on the method of Bejaoui *et al*. (2016) with slight modification. Plant material (0.5 g) was ground with 5 mL of TCA extract containing 0.25% thiobarbituric acid (TBA) and reacted at 100°C for 30 min. The supernatant was obtained by centrifugation

for 10 min at 10,000 × *g*, and the absorbance was recorded at 600, 532, and 450 nm. The amount of MDA in wheat leaves was presented as μM g^{-1}(FM).

Chloroplast suspension (1 mL) with an equal amount of Chl was sequentially mixed with distilled water (1.5 mL) and 20% TCA solution (2.5 mL) containing 0.5% TBA, bathed for 15 min in boiling water and cooled rapidly. The absorbance (450, 532, and 600 nm) of the supernatant obtained by centrifugation (10 min; 4,000 × *g*) was reported. An extinction coefficient of 155 mM^{-1} cm^{-1}, as described by Bejaoui *et al*. (2016), was used to compute the chloroplast MDA content, expressed as nmol mg^{-1}(Chl).

Chloroplast antioxidant enzyme activities: A chloroplast suspension with the same amount of Chl was added to 25 mM Hepes buffer (pH 7.8) supplemented with 2% polyvinyl pyrrolidone and 200 mM EDTA and then centrifuged (20 min; 12,000 × *g*) to obtain the supernatant for measuring the activities of antioxidant enzymes. All chloroplast antioxidant enzyme activities were expressed as U mg^{-1}(Chl).

Chloroplast SOD (EC 1.15.1.1) activity was analyzed by detecting the inhibition of the light chemical reduction capacity of NBT (Wang *et al*. 2018). A moderate amount of the supernatant was mixed with 50 mM PBS buffer (pH 7.8) with 13 mM methionine, 75 μM NBT, and 100 M EDTA-Na_2. The reaction was initiated using 2 μM riboflavin and performed for 30 min (25°C) under illumination. The absorbance at 560 nm was recorded. The enzyme dosage required for 50% inhibition of NBT reduction was confirmed as one unit of SOD activity.

The change in absorbance (470 nm) of guaiacol oxidation was documented to analyze chloroplast POD (EC 1.11.1.7) activity (Wu *et al*. 2018). An appropriate amount of the supernatant (containing 20–40 μg of Chl), 200 mM PBS buffer (pH 6.0), and 20 mM guaiacol were blended well together, and the reaction was activated with 0.25% H_2O_2. The absorbance (470 nm) was scanned for 3 min. The change in OD_{470nm} per min was defined as an enzyme activity unit (U).

The enzyme extract was added to the detection solution for APX (EC 1.11.1.11) consisting of PBS buffer (pH 7.0, 50 mM) and ascorbate (500 M), and the reaction lasted for 5 min (25°C) after the addition of 5% H_2O_2. The absorbance (290 nm) was scanned for 1 min, and one unit of enzyme activity was confirmed from the amount of APX catalyzing the oxidation of 1 μmol(ascorbate) per min (Dai and Shan 2019).

Chloroplast GR (EC 1.6.4.2) activity was analyzed by monitoring the decrease in absorbance (340 nm) resulting from nicotinamide adenine dinucleotide phosphate (NADPH) oxidation (Hasanuzzaman *et al*. 2012). The reaction system comprised 100 μM Tris-HCl (pH 7.8) with NADPH (50 μM), EDTA (2 mM), glutathione (500 μM), and appropriate enzyme extracts. The reaction system was incubated in the dark at 25°C for 5 min. OD_{340nm} was recorded every 30 s for 3 min, and the change within 1 min was determined as one unit of enzyme activity.

Real-time quantitative polymerase chain reaction: Wheat leaves were ground into a powder using liquid nitrogen and added to 1 mL of *RNAiso Plus* (*Takara*, Japan). Centrifugation (12,000 rpm, 10 min) was performed to gather the supernatant, supplemented with 200 μL of chloroform. After shaking and 10 min of incubation, centrifugation was repeated under identical conditions. Then, the RNA solution was mixed with an equal volume of pre-cooled isopropanol solution and incubated for 10 min. Following another round of centrifugation (10 min), the supernatant was decanted, and 650 μL of 75% ethanol solution (containing 0.1% DEPC) was added and thoroughly mixed. Centrifugation (8,000 rpm, 5 min) at 4°C was carried out. Ethanol was discarded and then further centrifuged for 5 min. Ethanol was discarded, and the tube was inverted on an ultra-clean bench, allowing the RNA to air-dry slightly. Subsequently, the precipitate was dissolved with RNase-free water (50 μL), yielding the total RNA. The RNA concentration was assessed after 30 min (*NanoDrop Technologies*, Wilmington, DE, USA).

The related sequences and specific primers of *TaFeSOD*, *TatAPX*, and *TaChlGR* were obtained from *NCBI* and *Primer Premier 5.0* software, respectively. Specific primers were synthesized by *Shanghai Shenggong Biological Engineering Co., Ltd*. The instructions of the *SYBR Premix Ex TaqTM Kit* were used to perform RT-PCR reactions. Three parallel genes were set in each treatment group and amplified by qPCR instrument (*QuantStudio™ 1 Plus*, *Thermo Fisher Scientific*, China), and gene expression was determined depending on the $2^{-\Delta\Delta Ct}$ method.

Primer	Sequence (5'–3')
TaGAPDH	F: TTAGACTTGCGAAGCCAGCA R: AAATGCCCTTGAGGTTTCCC
TaFeSOD	F: CCTACTGGATGAGACGGAGAG R: GGACGAGGACAACGACGAA
TatAPX	F: CCATGGCGGAGCGCATCG R: CCTGGAAAATGGTTAATTACA
TaChlGR	F: TTGGGCTGTTGGAGATGTTA R: TTGGGCTGTTGGAGATGTTA

Statistical and analysis of experimental data: At least four independent experiments were performed on the control and treated plants to analyze leaf area and biomass. Other indicators were assessed through at least three independent experiments involving the control and treatment groups. Statistical data were analyzed by applying software *Excel 2007* and *SPSS 17.0*, and the results were displayed as average value ± standard error (SE). One-way analysis of variance (*ANOVA*) using *Duncan*'s method was replicated for the analyses of variance and multiple comparisons. Significant differences between various treatments were indicated by lowercase letters, with significance determined at the $P<0.05$ level.

Results

Leaf area and biomass in wheat seedlings: Compared with the control, 50 μM Zn (low-concentration Zn) treatment

increased leaf area and stem DM by approximately 17 and 12%, respectively, and the other indicators did not change significantly. Notably, 250 μM Zn (high-concentration Zn) alone inhibited the growth of roots and stems as demonstrated by decreased FM and DM with reduced leaf area (Fig. 1*A–C*). The effects of 300 μM Fe stress were notably weaker than those of 500 μM Fe exposure (Fig. 1*C*,*D*). Compared with 300 μM Fe treatment alone, adding 50 μM Zn to Fe-treated seedlings significantly increased FM and DM of stems by approximately 16 and 40%, respectively, as well as markedly improved root FM and DM and leaf area. By contrast, the addition of 250 μM Zn to Fe-stressed ones only enhanced root DM by nearly 16%. Therefore, the alleviation of the Fe-inhibitory effect by 50 μM Zn was more pronounced than that by 250 μM Zn.

Photosynthetic gas-exchange parameters in wheat seedling leaves: With respect to the control, P_N, E, and g_s of wheat leaves were notably upregulated by 43, 87, and 37%, respectively, due to 50 μM Zn exposure alone (Fig. 2). In contrast, these three parameters were significantly downregulated under high-concentration Zn or Fe treatment alone, displaying a 39, 32, and 16% reduction due to 250 μM Zn. A respective decrease of 51, 53, and 50% due to 300 μM Fe, while 70, 68, and 70% reduction due to 500 μM Fe were found compared with the control. No significant difference in C_i was found between the control and those exposed to Zn or Fe alone. The application of 50 μM Zn partly mitigated the 300 μM Fe-induced decrease of P_N, E, and g_s but further downregulated C_i in Fe-stressed wheat leaves. Compared with 300 μM Fe exposure alone, 250 μM Zn application further weakened P_N, E, and C_i but effectively reversed the reduction in g_s in 300 μM Fe-stressed wheat leaves. For example, P_N of wheat leaves exposed to Fe alone was 2.22 ± 0.17 μmol(CO_2) m^{-2} s^{-1}, whereas that of leaves exposed to Fe + 250 μM Zn was 1.79 ± 0.06 μmol(CO_2) m^{-2} s^{-1}. The g_s for these conditions was 40.43 ± 1.41 and 69.03 ± 0.79 μmol m^{-2} s^{-1}, respectively.

Hill reaction and ATPase activities in wheat chloroplasts: The Hill reaction activity was unaffected by low-concentration Zn treatment. Still, it decreased to 52% of the control under high-concentration Zn treatment alone (Fig. 3*A*). Similar to high-concentration Zn, 300 or 500 μM Fe stress alone lowered the activity of the Hill reaction to 36 and 50% of the control, respectively. Compared with 300 μM Fe stress alone, low-concentration Zn enhanced the Hill reaction activity of chloroplasts in Fe-treated seedlings by nearly 27%. However, the addition of high-concentration Zn did not affect this parameter.

Mg^{2+}-ATPase activity remained unaltered by 50 μM Zn exposure alone but decreased by 24% at 250 μM Zn compared with the control. Individual treatment with 300 or 500 μM Fe weakened enzyme activity to 84 and 64% of the control, respectively (Fig. 3*B*). Moreover, slight

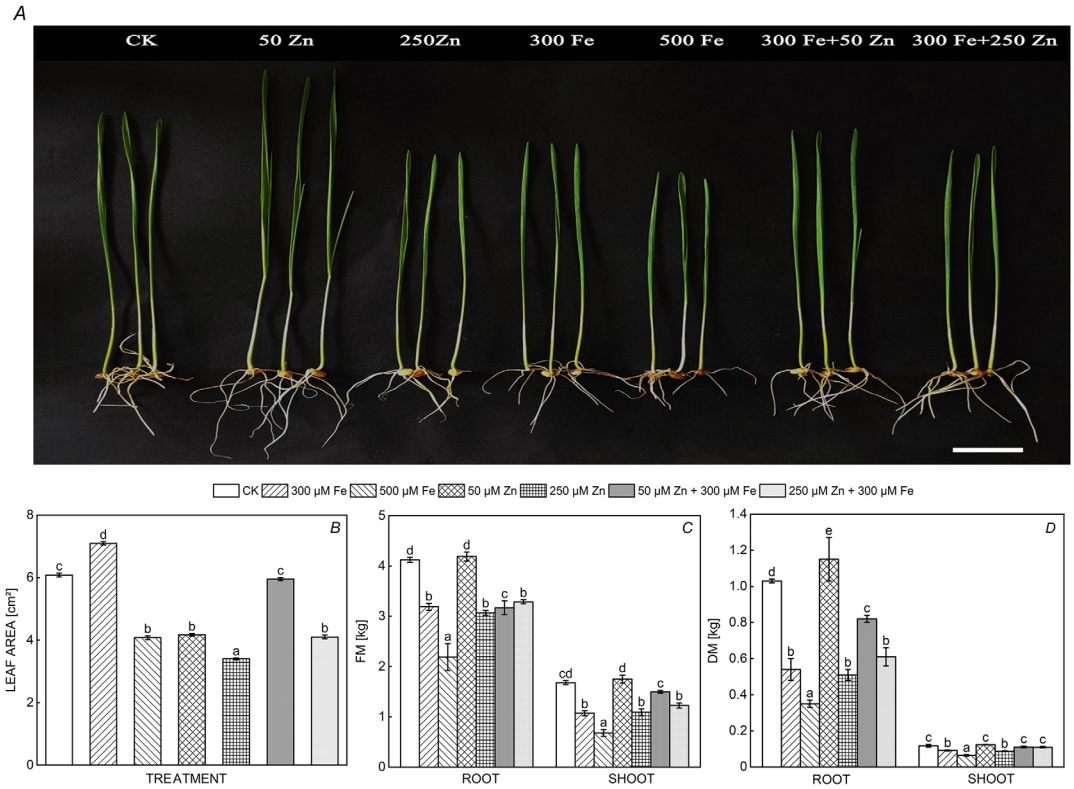

Fig. 1. Growth (*A*), leaf area (*B*), fresh mass (FM) (*C*), and dry mass (DM) (*D*) in wheat seedlings exposed to different treatments. Columns are the means of three replicates ± standard error (n = 3), and *different letters* above the error bars indicate significant difference (p<0.05).

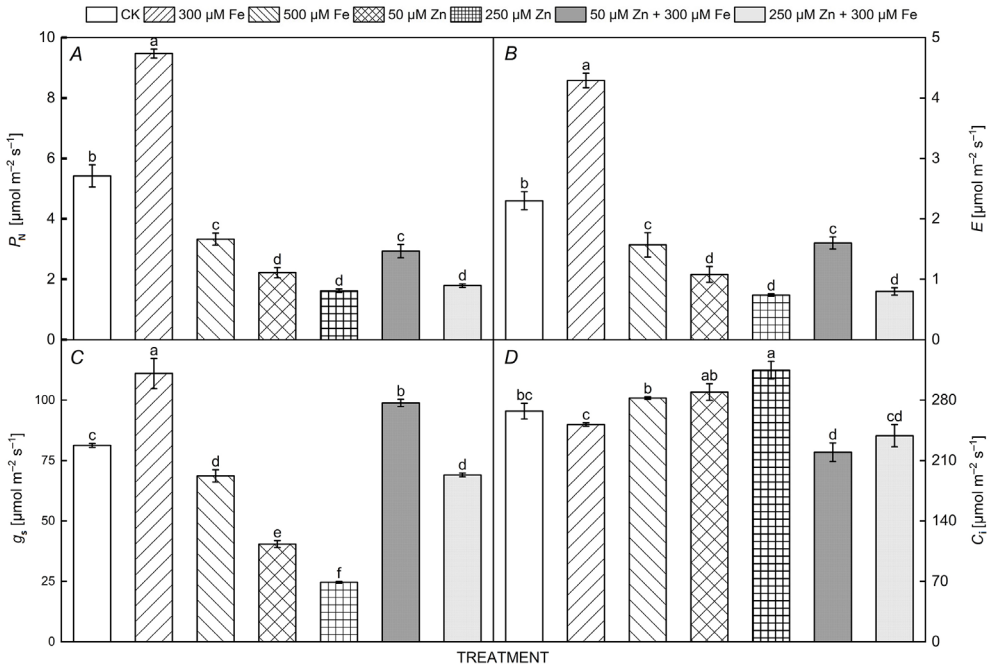

Fig. 2. Net photosynthetic rate (P_N) (*A*), transpiration rate (E) (*B*), stomatal conductance (g_s) (*C*), and intercellular CO_2 concentration (C_i) (*D*) in wheat leaves under different treatments. Columns are the means of three replicates ± standard error (n = 3), and *different letters* above the error bars indicate significant difference (p<0.05).

variations in Mg^{2+}-ATPase activity were observed between Fe-stressed and Fe + Zn-treated seedlings.

Ca^{2+}-ATPase activity in wheat chloroplast was upregulated by 13% under low-concentration Zn treatment but downregulated by 16% under high-concentration Zn exposure. Similar to high-concentration Zn treatment, 300 or 500 μM Fe stress alone suppressed chloroplast Ca^{2+}-ATPase activity by 20 and 32%, respectively, compared with the control. Low-concentration Zn supplement increased Ca^{2+}-ATPase activity in the chloroplasts of Fe-treated seedlings by 11%, whereas 250 μM Zn application did not affect enzyme activity, compared with 300 μM Fe alone (Fig. 3*C*).

H_2O_2 and $O_2^{\bullet-}$ contents in wheat leaves and chloroplasts: NBT staining showed that untreated and 50 μM Zn-treated leaves exhibited pale coloration with only a small number of blue spots, whereas an increased number of blue spots appeared in 250 μM Zn-stressed leaves (Fig. 4*A*). Fe stress also resulted in enhanced $O_2^{\bullet-}$ staining of wheat leaves compared with the control. The presence of 50 μM Zn reduced the blue spots on Fe-stressed leaves, but Fe-stressed leaves exposed to 250 μM Zn were nearly completely covered by blue spots compared with 300 μM Fe treatment.

A 20% reduction in chloroplast H_2O_2 content was found between the control and low-concentration Zn treatment, but no change was observed under high-concentration Zn exposure. By contrast, 300 or 500 μM Fe stress alone induced an obvious accumulation of chloroplast H_2O_2, which increased by 23 and 36% compared with the control, respectively. Low-concentration Zn application effectively prevented the Fe-induced increase of chloroplast H_2O_2 content, resulting in a 12% reduction compared with 300 μM Fe alone, whereas no significant difference was found between Fe stress alone and Fe + high-concentration Zn treatment (Fig. 4*C*).

By contrast, the formation rate of $O_2^{\bullet-}$ in the chloroplasts showed no notable change under low-concentration Zn treatment but increased by 37% under high-concentration Zn exposure. Similar to high-concentration Zn treatment, Fe stress alone at 300 or 500 μM significantly increased the formation rate of chloroplast $O_2^{\bullet-}$ to 130 and 173% of the control, respectively. Low or high concentrations of Zn did not affect the rate of chloroplast $O_2^{\bullet-}$ formation induced by 300 μM Fe stress (Fig. 4*D*).

Lipid peroxidation level in wheat leaves and chloroplasts: The MDA content in wheat leaves remained unaltered with 50 μM Zn treatment alone but increased by 58% with 250 μM Zn alone. Fe stress alone (300 or 500 μM) increased leaf MDA content to 161 and 188% of the control, respectively. Moreover, 50 μM Zn reduced the MDA content in the leaves of Fe-stressed seedlings by 33%, whereas the addition of high-concentration Zn elevated the MDA content by 48% compared with 300 μM Fe alone (Fig. 4*B*). Additionally, the MDA content in wheat leaves exposed to high-concentration Fe was more prominent than that in leaves exposed to high-concentration Zn.

Low-concentration Zn exposure alone did not affect the chloroplast MDA content, but high-concentration Zn treatment increased this parameter (Fig. 4*E*). The chloroplasts subjected to 300 or 500 μM Fe treatment

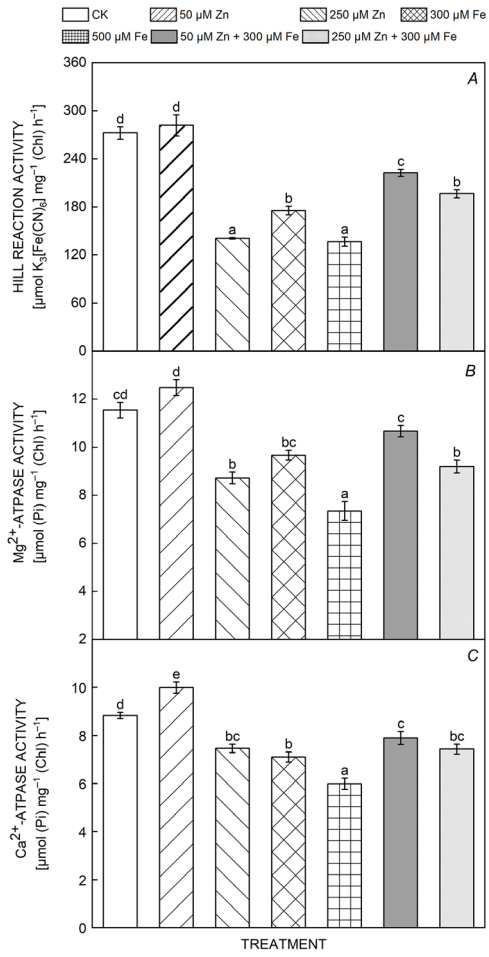

Fig. 3. Hill reaction (*A*), Mg^{2+}-ATPase (*B*), and Ca^{2+}-ATPase (*C*) activities in wheat chloroplast under different treatments. Columns are the means of three replicates ± standard error ($n = 3$), and *different letters* above the error bars indicate significant difference ($p<0.05$).

exhibited 2.7- and 3-fold increases in MDA contents, respectively, relative to the control. Moreover, the addition of Zn (50 or 250 μM) to Fe (300 μM)-stressed seedlings reduced the MDA content by 44 and 27%, respectively, compared with the 300 μM Fe treatment alone.

Antioxidant enzyme activities in wheat chloroplasts: The activity of chloroplast SOD slightly changed under 50 μM Zn treatment, but notably rose to 1.23-fold of the control under high-concentration Zn exposure. Treatment with 300 or 500 μM Fe alone stimulated chloroplast SOD activity to 30 and 50% of the control, respectively. Compared with individual Fe (300 μM) treatment, the addition of low-concentration Zn to Fe (300 μM)-treated wheat seedlings downregulated the activity of chloroplast SOD by about 15%, whereas high-concentration Zn did not affect this enzyme activity (Fig. 5*A*).

The change in chloroplast POD activity differed in response to two Zn concentrations. Compared with the control, the enzyme activity of low-concentration Zn treatment decreased by 21%, whereas that of 250 μM Zn exposure remained unaltered. By contrast, 300 or 500 μM Fe stress alone upregulated the enzyme activity to 125 and 161% of the control, respectively. Additionally, the Zn supplement did not modify chloroplast POD activity in Fe-stressed seedlings (Fig. 5*B*).

The activity of chloroplast APX lowered first and then rose under Zn treatment (Fig. 5*C*). Compared with the control, enzyme activity was downregulated by 21% under 50 μM Zn treatment but upregulated by 17% under 250 μM Zn exposure. Similar to high-concentration Zn treatment, exposure to 300 or 500 μM Fe alone stimulated chloroplast APX activity by 29 and 80%, respectively, compared with the control. A notable decrease in chloroplast APX activity was observed between Fe stress alone and Fe + low-concentration Zn treatment, whereas the addition of high-concentration Zn did not alter this parameter in wheat seedlings exposed to Fe.

Chloroplast GR activity altered insignificantly under different concentrations of Zn or low-concentration Fe treatment, whilst 500 μM Fe stress alone notably upregulated this enzyme activity by 43%. Moreover, we found no significant difference in chloroplast GR activity between 300 μM Fe stress alone and Fe + high-concentration Zn treatment (Fig. 5*D*).

Antioxidant enzyme gene expression in wheat chloroplast: The expression of *TaFeSOD* exhibited no changes following 50 μM Zn treatment alone for 2 d but decreased to 73% of the control after treatment for 6 d. However, *TaFeSOD* expression increased by 4.42- and 8.04-fold when wheat leaves were treated with high-concentration Zn alone for 2 and 6 d, respectively. Similar to high-concentration Zn, Fe exposure at both concentrations significantly upregulated the expression of this gene. For example, *TaFeSOD* expression under 500 μM Fe exposure alone for 2 and 6 d increased to 8.13 and 8.81 times the control, respectively. Compared with 300 μM Fe alone, *TaFeSOD* expression decreased by 82 and 87% under composite treatment of Fe and low-concentration Zn for 2 and 6 d, respectively but it was upregulated under combined exposure of Fe (300 μM) and high-concentration Zn for the same durations (Fig. 6*A*).

TatAPX expression under different treatments is shown in Fig. 6*B*. Low-concentration Zn treatment for 2 and 6 d significantly inhibited *TatAPX* expression in wheat leaves, by 23 and 73%, respectively, compared with the control. Conversely, high-concentration Zn treatment resulted in a markedly upregulated *TatAPX* expression to 4.08- and 3.69-fold of the control at 2 and 6 d, whereas high-concentration Fe treatment increased it to 5.98- and 5.56-fold of the control for the same duration. Low-concentration Zn supplementation significantly downregulated the expression of *TatAPX* by 86 and 94% under 2 and 6 d of Fe stress, respectively, whereas the high-concentration Zn notably enhanced this gene expression by 41 and 57% at 2 and 6 d of Fe treatment, respectively, compared with 300 μM Fe stress alone.

The expression of *TachlGR* was notably downregulated under 50 μM Zn treatment alone for 2 and 6 d, whereas

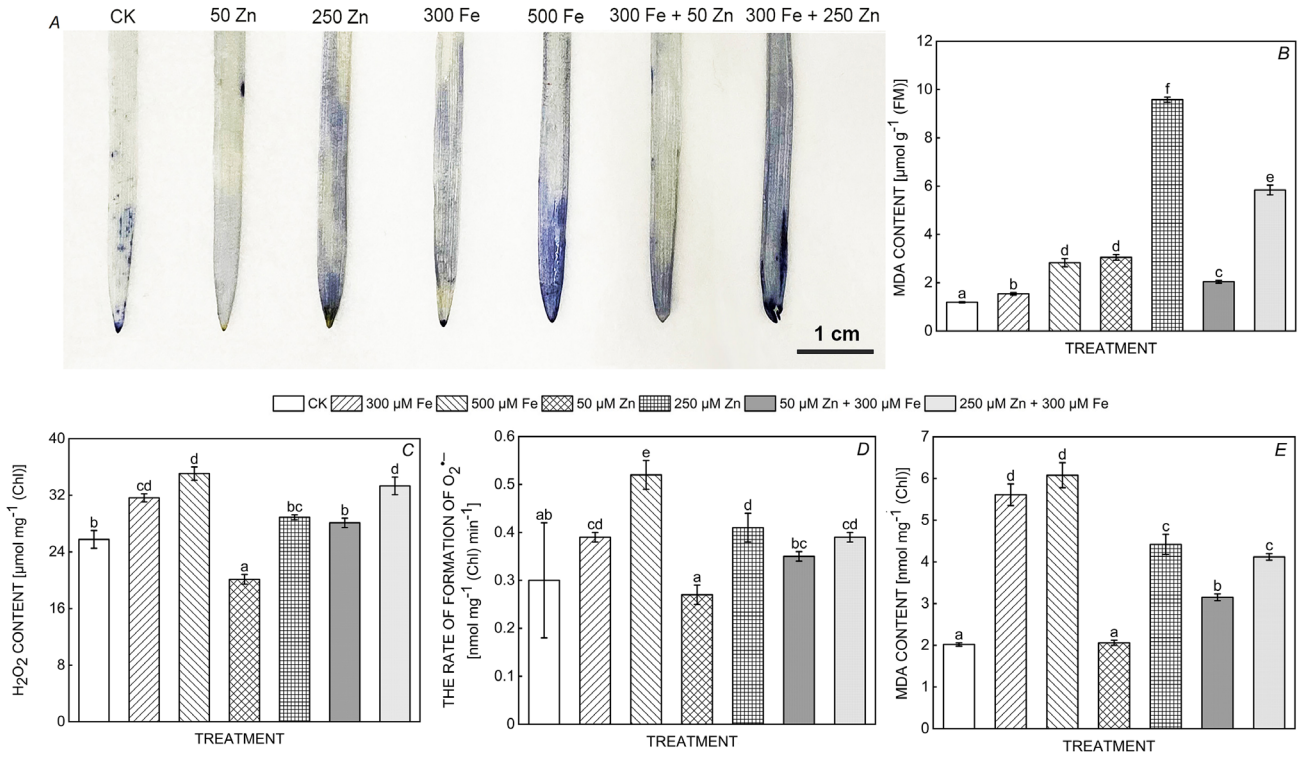

Fig. 4. Nitroblue tetrazolium (NBT) staining (*A*) and malondialdehyde (MDA) content (*B*) of wheat leaves, H_2O_2 (*C*), $O_2^{\bullet-}$(*D*), and MDA (*E*) contents in wheat chloroplast under different treatments. Columns are the means of three replicates ± standard error ($n = 3$), and *different letters* above the error bars indicate significant difference ($p<0.05$).

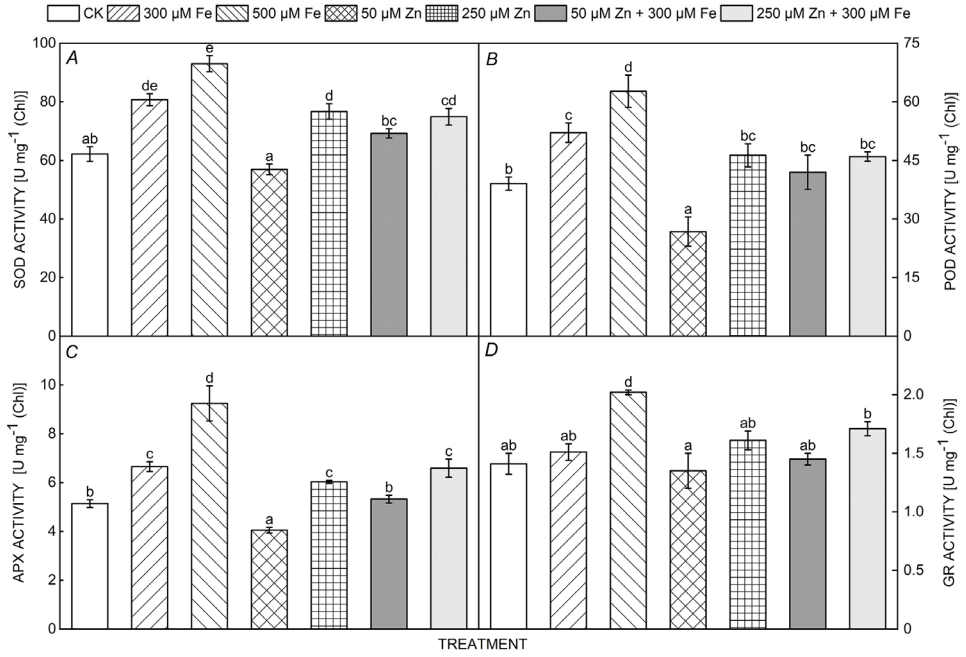

Fig. 5. Superoxide dismutase (SOD) (*A*), peroxidase (POD) (*B*), ascorbate peroxidase (APX) (*C*), and glutathione reductase (GR) (*D*) activities in wheat chloroplast under different treatments. Columns are the means of three replicates ± standard error ($n = 3$), and *different letters* above the error bars indicate significant difference ($p<0.05$).

250 μM Zn and Fe (300 and 500 μM) exposure alone significantly upregulated this gene expression. For example, the expression of *TaChlGR* under low-concentration Zn treatment for 2 and 6 d decreased to 61 and 35% of the control, respectively. By contrast, this gene expression under 250 μM Zn treatment for 2 and 6 d increased

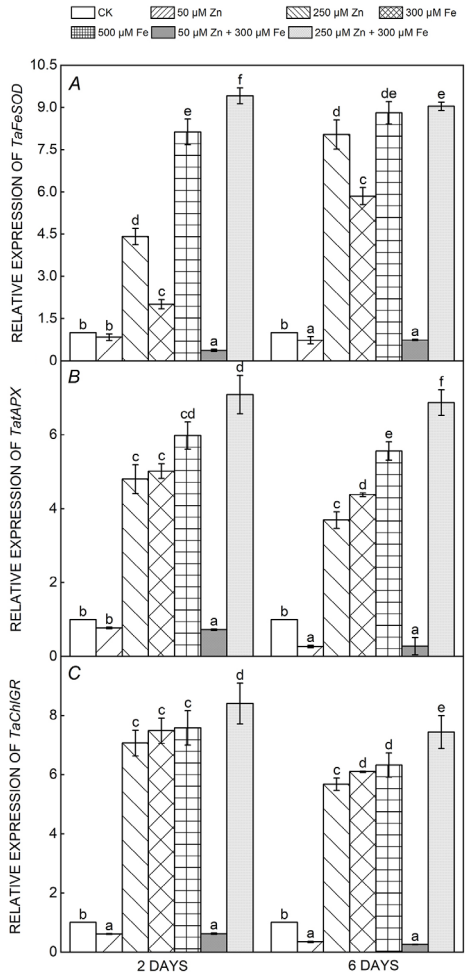

Fig. 6. The expression of antioxidant enzyme genes in wheat chloroplast under different treatments. Columns are the means of three replicates ± standard error (n = 3), and *different letters* above the error bars indicate significant difference (p<0.05).

by 6.07 and 4.68 times, respectively, compared with the control. The addition of low-concentration Zn to Fe (300 μM)-treated wheat seedlings reduced the expression of *TaChlGR* by 92 and 96% at 2 and 6 d. Conversely, the gene expression under the combined exposure of Fe (300 μM) and Zn (low concentration) for 2 and 6 d increased by 1.12 and 1.22 times, respectively, compared with the 300 μM Fe treatment alone (Fig. 6*C*).

Discussion

The detrimental effects of heavy metal contamination on plants generally present reduced biomass and inhibited growth (Chen *et al*. 2020, Zhang *et al*. 2020a). Our recent observations showed that appropriate Zn application promoted the growth of wheat roots and shoots, but elevated concentrations of Zn or Fe hindered growth (Yang *et al*. 2021). The variation in leaf area, root, and shoot biomass (Fig. 1*D*) in this experiment further supported the results on wheat seedling growth under Zn or Fe treatment. Other studies have also reported analogous changes in leaf area, biomass, and growth across various plant species subjected to different concentrations of Zn or Fe (Du *et al*. 2019, Gindri *et al*. 2020, Wang *et al*. 2021, Tisarum *et al*. 2023), suggesting that low concentrations of Zn enhanced plant growth, but high concentrations of Zn or Fe treatment induced phytotoxicity, thereby inhibiting plant growth. Photosynthesis is crucial for plant growth and crop yield (Kang *et al*. 2017), and its susceptibility to abiotic stress can impede plant development (Mateos-Naranjo *et al*. 2013, Du *et al*. 2016, Hu *et al*. 2022). The notable upregulation or downregulation of P_N, E, and g_s under different concentrations of Zn or Fe treatment, along with the marked increase in C_i due to 500 μM Fe stress, indicated that low-concentration Zn promoted photosynthesis *via* stomatal and nonstomatal mechanisms in wheat leaves. Similar photosynthetic capacity and damage to the photosynthetic apparatus were observed in various plants subjected to Zn or Fe treatment (Yang *et al*. 2021, Li *et al*. 2022). The Zn-alleviating effect on growth inhibition has been noted in Pb-stressed *Alcea rosea* (Linn.) Cavan. (Duan *et al*. 2022) and Cd-stressed wheat (Sarwar *et al*. 2015), as well as in mercury-treated *Pfaffia glomerata* plantlets (Calgaroto *et al*. 2011). Moreover, our recent study demonstrated Zn's mitigating impact on Fe toxicity associated with root and leaf lengths of wheat seedlings (Yang *et al*. 2021). This effect was further supported by the increase in leaf area and seedling biomass in Zn + Fe-exposed wheat seedlings compared with that in seedlings subjected to Fe alone. Consequently, there is an urgent need to explore the ways and mechanisms of improving photosynthetic efficiency and promoting plant growth for crop quality under high-concentration Fe environments. Notably elevated P_N, E, and g_s may lead to enhanced carbon inputs and sugar synthesis in Zn (50 μM) + Fe-treated wheat seedlings, whereas Zn (250 μM) + Fe treatment further decreased P_N and C_i but increased E. Therefore, the prudent application of Zn is beneficial in mitigating Fe toxicity from hindering seedling growth by disrupting the photosynthetic system.

Given that photophosphorylation is a limiting factor for photosynthesis, the analysis of chloroplast Hill reaction efficacy and ATPase activity associated with plant photophosphorylation (Huang *et al*. 2008, Hu *et al*. 2016, Fu *et al*. 2018) is essential for wheat seedling growth under different Zn and Fe treatments. Various studies have highlighted the significant reduction in chloroplast Hill reaction and ATPase activity and the concurrent inhibition of photosynthesis in diverse plant species under different abiotic environments (Wu *et al*. 2008, Fu *et al*. 2018, Das and Biswas 2022). In rice chloroplasts, the activity of Mg^{2+}-ATPase and the transcription of ATPase subunits were notably enhanced with the increase in P_N and plant growth under low lanthanum concentrations, while these parameters declined with the degradation of the chloroplast ultrastructure under elevated La contents (Hu *et al*. 2016). Similar to low-concentration La exposure, the augmentation of the vitality of the Hill reaction and the activities of Mg^{2+}-ATPase and Ca^{2+}-ATPase in chloroplasts suggested an enhancement of photosynthetic phosphorylation and, consequently, an elevation in photosynthesis in wheat

seedlings exposed to low concentrations of Zn. This phenomenon may contribute to the observed promotion of wheat seedling growth induced by low-concentration Zn. However, other studies, together with the attenuation of the Hill reaction, Mg^{2+}-ATPase, and Ca^{2+}-ATPase in plant chloroplasts collectively affirmed the disruption of chloroplast structure and a reduction in photosynthesis, thereby inhibiting wheat seedlings under excessive Zn or Fe stresses. No correlation has been found between photophosphorylation and plant growth concerning the alleviation of heavy metal toxicity. Intriguingly, in Fe-stressed wheat leaves, adding 50 μM Zn effectively mitigated the inhibitory effects of Fe on the chloroplast Hill reaction and Ca^{2+}-ATPase activity, whereas the application of 250 μM Zn had a negligible impact on these parameters. These results implied that appropriate Zn application could enhance plant photosynthesis by alleviating the reduction of photosynthetic phosphorylation in the chloroplasts of Fe-exposed wheat seedlings.

The chloroplast is the main site of photosynthesis and the main organelle of ROS generation (Zhou *et al.* 2018). In plant cells, a series of antioxidant enzymes at the subcellular level plays a crucial function in scavenging ROS under environmental stress (Fan *et al*. 2020). Salt stress weakened SOD, POD, APX, and GR activities and increased MDA content and $O_2^{\bullet-}$ generation in the chloroplasts of *Cucumis sativus* L. (Shu *et al*. 2013). Furthermore, the $LaCl_3$ pretreatment-induced upregulation of GR, APX, and SOD activities effectively reduced H_2O_2 and MDA contents in maize chloroplasts under Cr stress (Dai and Shan 2019). Additionally, exogenous spermine remarkably stimulated SOD, POD, and APX, thereby reducing $O_2^{\bullet-}$ and MDA contents in the salt-stressed chloroplasts of *C. sativus* L. (Shu *et al*. 2013). This result demonstrated that the synergistic action of antioxidant enzymes SOD, POD, and APX was crucial in preventing excessive accumulation of ROS and subsequent oxidative damage to plant chloroplasts (Zhang *et al*. 2020b). In the present study, under high-concentration Zn or Fe stress alone, increased H_2O_2, $O_2^{\bullet-}$, and MDA contents in wheat chloroplasts corresponded to a notable enhancement in the activities of chloroplast SOD, POD, or/and APX and their gene expression. This result agreed with recent observations indicating an increase in ROS contents together with the stimulation of antioxidant enzymes in the chloroplasts of salinity-stressed tomato (Zhang *et al*. 2016) and As-stressed maize (Elbasan *et al*. 2024). The enhanced antioxidant enzyme activities are insufficient to eliminate the excessive formation of ROS, resulting in oxidative damage to the chloroplasts and a reduction in photosynthesis in wheat seedlings under high-concentration Zn or Fe stress. However, reduced H_2O_2 generation in wheat chloroplasts was accompanied by downregulated chloroplast POD and APX activities and *TaFeSOD*, *TatAPX*, and *TaChlGR* expression levels under low-concentration Zn treatment. These findings confirmed that *TaFeSOD*, *TatAPX*, and *TaChlGR* expression levels were responsible for their enzymes in the chloroplasts of seedlings treated with Fe or Zn alone. The remarkably upregulated SOD activity in the leaves of *Potamogeton crispus* L. is attributed to increased *PcSOD* expression induced by increased $O_2^{\bullet-}$ production (Yang *et al*. 2011). Concerning Fe stress alone, decreased H_2O_2 content was consistent with the downregulation of SOD activity and *TaFeSOD* expression under the combined treatment of Zn (50 μM) + Fe (300 μM). Insignificant changes in H_2O_2 and $O_2^{\bullet-}$ were associated with stable antioxidant enzyme activities under combined exposure to Zn (250 μM) + Fe (300 μM). The positive correlation between SOD, POD, and APX activities and H_2O_2 production under different treatments suggested that these enzyme activities in wheat chloroplasts may be regulated by ROS production. This conjecture is supported by some researchers who reported that the stimulation of SOD, POD, CAT, and APX is accompanied by increased ROS production in various plants under adverse conditions (Anjum *et al*. 2016, Zhang *et al*. 2020b). Notably, Cao *et al* (2015) confirmed that increased H_2O_2 and O_2 concentrations function as signaling molecules that activate SOD and APX in the chloroplasts of tomato leaves during the early stages of drought stress. Unlike the uniformity of antioxidant enzyme activity and ROS production in this study, Si application lowers ROS contents but increases SOD and APX activities during the late stage of drought stress in the chloroplasts of tomato leaves (Cao *et al*. 2015). In contrast to individual Fe or Zn exposure alone, the combined treatment of Fe + 250 μM Zn resulted in a substantial upregulation of *TaFeSOD*, *TatAPX*, and *TaChlGR* expressions levels but the activities of SOD, APX, and GR in wheat chloroplasts remained unchanged. Inconsistencies between enzyme activity and gene expression have been reported also in other studies. For example, the downregulation of SOD and APX activities is correlated with the upregulation of *PeCu/Zn SOD* and *PeAPX2* expression in NaCl-stressed *Populus euphratica* Oliv. (Feng *et al*. 2022), and atrazine toxicity enhances APX, POD, and SOD activities but lowers these enzyme gene transcripts in Ca-treated *Pennisetum* seedlings (Erinle *et al*. 2016). Few studies assessed the relationship between antioxidant enzyme activity and gene expression in plant chloroplasts under heavy metal stress. These different and sometimes contradictory changes in enzyme activity and gene expression indicate that abiotic stress alters enzyme activity at the transcriptional and posttranscriptional levels, as well as directly affecting enzyme proteins to influence their activity (Ciarkowska *et al*. 2016).

Conclusion: Low-concentration Zn promoted the growth of wheat seedlings, whereas high-concentration Zn or Fe negatively affected seedling growth. Notably, the application of 50 μM Zn significantly bolstered the growth of wheat seedlings exposed to Fe treatment. This was achieved through the enhancement of photosynthesis, Hill reaction, and ATPase activities, along with the reduction of ROS production and the consequential mitigation of peroxidation damage. By contrast, 250 μM Zn exhibited a weak alleviating effect on Fe toxicity within wheat chloroplasts. Exploring the mechanism of Zn-alleviating plant Fe toxicity has important significance for improving the quality of crops in Fe-contaminated

soil. Therefore, these Zn concentrations are recommended for the growth of wheat plants, and the application of appropriate Zn concentrations must be evaluated under field conditions.

References

Adil M.F., Sehar S., Han Z.G. *et al*.: Zinc alleviates cadmium toxicity by modulating photosynthesis, ROS homeostasis, and cation flux kinetics in rice. – Environ. Pollut. **265**: 114979, 2020.

Anjum S.A., Tanveer M., Hussain S. *et al*.: Osmoregulation and antioxidant production in maize under combined cadmium and arsenic stress. – Environ. Sci. Pollut. Res. **23**: 11864-11875, 2016.

Bejaoui F., Salas J.J., Nouairi I. *et al*.: Changes in chloroplast lipid contents and chloroplast ultrastructure in *Sulla carnosa* and *Sulla coronaria* leaves under salt stress. – J. Plant Physiol. **198**: 32-38, 2016.

Briat J.-F., Dubos C., Gaymard F.: Iron nutrition, biomass production, and plant product quality. – Trends Plant Sci. **20**: 33-40, 2015.

Calgaroto N.S., Cargnelutti D., Rossato L.V. *et al.*: Zinc alleviates mercury-induced oxidative stress in *Pfaffia glomerata* (Spreng.) Pedersen. – BioMetals **24**: 959-971, 2011.

Cao B.L., Ma Q., Zhao Q. *et al*.: Effects of silicon on absorbed light allocation, antioxidant enzymes and ultrastructure of chloroplasts in tomato leaves under simulated drought stress. – Sci. Hortic.-Amsterdam **194**: 53-62, 2015.

Chatterjee A.K., Mandal B., Mandal L.N.: Interaction of nitrogen and potassium with zinc in submerged soil and lowland rice. – J. Indian Soc. Soil Sci. **44**: 792-794, 1996.

Chen H.-C., Zhang S.-L., Wu K.-J. *et al*.: The effects of exogenous organic acids on the growth, photosynthesis and cellular ultrastructure of *Salix variegata* Franch. under Cd stress. – Ecotox. Environ. Safe. **187**: 109790, 2020.

Ciarkowska A., Ostrowski M., Jakubowska A.: Abiotic stress and phytohormones affect enzymic activity of 1-*O*-(indole-3-acetyl)-β-D-glucose: *myo*-inositol indoleacetyl transferase from rice (*Oryza sativa*). – J. Plant Physiol. **205**: 93-96, 2016.

Dai H., Shan C.: Effects of lanthanum on the antioxidant capacity of chloroplasts and chlorophyll fluorescence parameters of maize seedlings under chromium stress. – Photosynthetica **57**: 27-31, 2019.

Das S., Biswas A.K.: Comparative study of silicon and selenium to modulate chloroplast pigments levels, Hill activity, photosynthetic parameters and carbohydrate metabolism under arsenic stress in rice seedlings. – Environ Sci. Pollut. Res. **29**: 19508-19529, 2022.

Delias D.S., Da-Silva C.J., Martins A.C. *et al*.: Iron toxicity increases oxidative stress and impairs mineral accumulation and leaf gas exchange in soybean plants during hypoxia. – Environ. Sci. Pollut. Res. **29**: 22427-22438, 2022.

Ding F., Wang M., Zhang S.: Overexpression of a Calvin cycle enzyme SBPase improves tolerance to chilling-induced oxidative stress in tomato plants. – Sci. Hortic.-Amsterdam **214**: 27-33, 2017.

Du J., Shu S., Shao Q.S. *et al*.: Mitigative effects of spermidine on photosynthesis and carbon-nitrogen balance of cucumber seedlings under $Ca(NO_3)_2$ stress. – J. Plant Res. **129**: 79-91, 2016.

Du J., Zeng J., Ming X.Y. *et al*.: The presence of zinc reduced cadmium uptake and translocation in *Cosmos bipinnatus* seedlings under cadmium/zinc combined stress. – Plant Physiol. Biochem. **151**: 223-232, 2020.

Du W., Yang J.Y., Peng Q.Q. *et al*.: Comparison study of Zn nanoparticles and Zn sulphate on wheat growth: from toxicity and Zn biofortification. – Chemosphere **227**: 109-116, 2019.

Duan Y.P., Zhang Y., Zhao B.: Lead, zinc tolerance mechanism and phytoremediation potential of *Alcea rosea* (Linn.) Cavan. and *Hydrangea macrophylla* (Thunb.) Ser. and ethylenediaminetetraacetic acid effect. – Environ. Sci. Pollut. Res. **29**: 41329-41343, 2022.

Elbasan F., Arikan B., Ozfidan-Konakci C. *et al*.: Hesperidin and chlorogenic acid mitigate arsenic-induced oxidative stress via redox regulation, photosystems-related gene expression, and antioxidant efficiency in the chloroplasts of *Zea mays*. – Plant Physiol. Biochem. **208**: 108445, 2024.

Erinle O.K., Jiang Z., Ma B.B. *et al*.: Exogenous calcium induces tolerance to atrazine stress in *Pennisetum* seedlings and promotes photosynthetic activity, antioxidant enzymes and *psbA* gene transcripts. – Ecotox. Environ. Safe. **132**: 403-412, 2016.

Fan W.-J., Feng Y.-X., Li Y.-H. *et al*.: Unraveling genes promoting ROS metabolism in subcellular organelles of *Oryza sativa* in response to trivalent and hexavalent chromium. – Sci. Total Environ. **744**: 140951, 2020.

Feng K., Lu J., Chen Y. *et al*.: The coordinated alterations in antioxidative enzymes, *PeCu/ZnSOD* and *PeAPX2* expression facilitated in vitro *Populus euphratica* resistance to salinity stress. – Plant Cell Tiss. Org. Cult. **150**: 399-416, 2022.

Fu J., Wang Y.-F., Liu Z.-H. *et al*.: *Trichoderma asperellum* alleviates the effects of saline–alkaline stress on maize seedlings via the regulation of photosynthesis and nitrogen metabolism. – Plant Growth Regul. **85**: 363-374, 2018.

Gindri R.G., Navarro B.B., da Cruz Dias P.V. *et al*.: Physiological responses of rice (*Oryza sativa* L.) *oszip*7 loss-of-function plants exposed to varying Zn concentrations. – Physiol. Mol. Biol. Pla. **26**: 1349-1359, 2020.

Hasanuzzaman M., Hossain M.A., Fujita M. *et al*.: Exogenous selenium pretreatment protects rapeseed seedlings from cadmium-induced oxidative stress by upregulating antioxidant defense and methylglyoxal detoxification systems. – Biol. Trace Elem. Res. **149**: 248-261, 2012.

Hu C.-H., Zheng Y., Tong C.-L., Zhang D.-J.: Effects of exogenous melatonin on plant growth, root hormones and photosynthetic characteristics of trifoliate orange subjected to salt stress. – Plant Growth Regul. **97**: 551-558, 2022.

Hu H., Wang L., Li Y. *et al*.: Insight into mechanism of lanthanum (III) induced damage to plant photosynthesis. – Ecotox. Environ. Safe. **127**: 43-50, 2016.

Huang H., Liu X.Q., Qu C.H. *et al*.: Influences of calcium deficiency and cerium on the conversion efficiency of light energy of spinach. – BioMetals **21**: 553-561, 2008.

Kang J.J., Zhao W.Z., Zheng Y. *et al*.: Calcium chloride improves photosynthesis and water status in the C_4 succulent xerophyte *Haloxylon ammodendron* under water deficit. – Plant Growth Regul. **82**: 467-478, 2017.

Kaur N., Sharma I., Kirat K., Pati P.K.: Detection of reactive oxygen species in *Oryza sativa* L. (rice). – Bio-protocol **6**: e2061, 2016.

Kroh G.E., Pilon M.: Regulation of iron homeostasis and use in chloroplasts. – Int. J. Mol. Sci. **21**: 3395, 2020.

Krohling C.A., Eutrópio F.J., Bertolazi A.A. *et al*.: Ecophysiology of iron homeostasis in plants. – Soil Sci. Plant Nutr. **62**: 39-47, 2016.

Li M.P., Kim C.H.: Chloroplast ROS and stress signaling. – Plant Commun. **3**: 100264, 2022.

Li S.-P., Zeng L.-S., Su Z.-L.: Wheat growth, photosynthesis and physiological characteristics under different soil Zn levels. – J. Integr. Agr. **21**: 1927-1940, 2022.

Li X., Ma H., Jia P. *et al.*: Responses of seedling growth and antioxidant activity to excess iron and copper in *Triticum aestivum* L. – Ecotox. Environ. Safe. **86**: 47-53, 2012.
Ma T., Duan X.H., Yang Y.Y. *et al.*: Zn-alleviating effects on Fe-induced phytotoxicity in roots of *Triticum aestivum*. – Biol. Plantarum **61**: 733-740, 2017.
Marschner P.: Marschner's Mineral Nutrition of Higher Plants. 3rd Edition. Pp. 672. Academic Press, Amsterdam 2012.
Mateos-Naranjo E., Andrades-Moreno L., Cambrollé J., Perez-Martin A.: Assessing the effect of copper on growth, copper accumulation and physiological responses of grazing species *Atriplex halimus*: ecotoxicological implications. – Ecotox. Environ. Safe. **90**: 136-142, 2013.
Mira M.M., Asmundson B., Renault S. *et al.*: Suppression of the soybean (*Glycine max*) *Phytoglobin GmPgb1* improves tolerance to iron stress. – Acta Physiol. Plant. **43**: 147, 2021.
Müller B.: Iron transport mechanisms and their evolution focusing on chloroplasts. – J. Plant Physiol. **288**: 154059, 2023.
Omoto E., Nagao H., Taniguchi M., Miyake H.: Localization of reactive oxygen species and change of antioxidant capacities in mesophyll and bundle sheath chloroplasts of maize under salinity. – Physiol. Plantarum **149**: 1-12, 2013.
Romanowska E., Drożak A., Pokorska B. *et al.*: Organization and activity of photosystems in the mesophyll and bundle sheath chloroplasts of maize. – J. Plant Physiol. **163**: 607-618, 2006.
Sarwar N., Ishaq W., Farid G. *et al.*: Zinc–cadmium interactions: Impact on wheat physiology and mineral acquisition. – Ecotox. Environ. Safe. **122**: 528-536, 2015.
Sharma P., Chouhan R., Bakshi P. *et al.*: Amelioration of chromium-induced oxidative stress by combined treatment of selected plant-growth-promoting rhizobacteria and earthworms *via* modulating the expression of genes related to reactive oxygen species metabolism in *Brassica juncea.* – Front. Microbiol. **13**: 802512, 2022.
Shu S., Yuan L.-Y., Guo S.-R. *et al.*: Effects of exogenous spermine on chlorophyll fluorescence, antioxidant system and ultrastructure of chloroplasts in *Cucumis sativus* L. under salt stress. – Plant Physiol. Biochem. **63**: 209-216, 2013.
Tisarum R., Rika R., Pipatsitee P. *et al.*: Iron (Fe) toxicity, uptake, translocation, and physio-morphological responses in *Catharanthus roseus.* – Physiol. Mol. Biol. Pla. **29**: 1289-1299, 2023.
van Oort P.A.J.: Mapping abiotic stresses for rice in Africa: Drought, cold, iron toxicity, salinity and sodicity. – Field Crop. Res. **219**: 55-75, 2018.
Wang G.P., Zhang X.Y., Li F. *et al.*: Overaccumulation of glycine betaine enhances tolerance to drought and heat stress in wheat leaves in the protection of photosynthesis. – Photosynthetica **48**: 117-126, 2010.
Wang J., Zhong X., Zhu K. *et al.*: Reactive oxygen species, antioxidant enzyme activity, and gene expression patterns in a pair of nearly isogenic lines of nicosulfuron-exposed waxy maize (*Zea mays* L.). – Environ. Sci. Pollut. Res. **25**: 19012-19027, 2018.
Wang J.H., Moeen-ud-din M., Yang S.H.: Dose-dependent responses of *Arabidopsis thaliana* to Zn are mediated by auxin homeostasis and transport. – Environ. Exp. Bot. **189**: 104554, 2021.
Wu C., Dun Y., Zhang Z.J. *et al.*: Foliar application of selenium and zinc to alleviate wheat (*Triticum aestivum* L.) cadmium toxicity and uptake from cadmium-contaminated soil. – Ecotox. Environ. Safe. **190**: 110091, 2019.
Wu J., Shu S., Li C. *et al.*: Spermidine-mediated hydrogen peroxide signaling enhances the antioxidant capacity of salt-stressed cucumber roots. – Plant Physiol. Biochem. **128**: 152-162, 2018.
Wu X., Liu C., Qu C.X. *et al.*: Effects of lead on activities of photochemical reaction and key enzymes of carbon assimilation in spinach chloroplast. – Biol. Trace Elem. Res. **126**: 269-279, 2008.
Yang H.Y., Shi G.X., Xu Q.S., Wang H.X.: Cadmium effects on mineral nutrition and stress related indices in *Potamogeton crispus*. – Russ. J. Plant Physiol. **58**: 253-260, 2011.
Yang Y.L., Xu Y.L., Li J.M. *et al.*: [Comparison of photosynthetic characteristics of wheat seedlings under Zn and Fe treatments alone or in combination.] – J. Lanzhou Univ. (Nat. Sci.) **57**: 344-352, 2021. [In Chinese]
Zhang C.Y., He Q., Wang M.H. *et al.*: Exogenous indole acetic acid alleviates Cd toxicity in tea (*Camellia sinensis*). – Ecotox. Environ. Safe. **190**: 110090, 2020a.
Zhang G.-H., Xu Q., Zhu X.-D. *et al.*: SHALLOT-LIKE1 is a KANADI transcription factor that modulates rice leaf rolling by regulating leaf abaxial cell development. – Plant Cell **21**: 719-735, 2009.
Zhang H.H., Li X., Xu Z.S. *et al.*: Toxic effects of heavy metals Pb and Cd on mulberry (*Morus alba* L.) seedling leaves: Photosynthetic function and reactive oxygen species (ROS) metabolism responses. – Ecotox. Environ. Safe. **195**: 110469, 2020b.
Zhang Z., Chang X.X., Zhang L. *et al.*: Spermidine application enhances tomato seedling tolerance to salinity-alkalinity stress by modifying chloroplast antioxidant systems. – Russ. J. Plant Physiol. **63**: 461-468, 2016.
Zhou Y., Diao M., Cui J.-X. *et al.*: Exogenous GSH protects tomatoes against salt stress by modulating photosystem II efficiency, absorbed light allocation and H_2O_2-scavenging system in chloroplasts. – J. Integr. Agr. **17**: 2257-2272, 2018.